DETERMINATION OF SNOW DEPTH USING ELEVATION DIFFERENCES DETERMINED BY INTERFEROMETRIC SAR (INSAR)

Jack R. Evans[1,♦] and Fred A. Kruse[2]

[1]Department of Meteorology, Naval Postgraduate School, Monterey, CA 93943
[2]Physics Department and Remote Sensing Center, Naval Postgraduate School, Monterey, CA 93943

ABSTRACT

Snow accumulation is a significant factor for determining sources and amounts of seasonal runoff for a variety of applications. Most current estimates of snow depth, however, consist of manual (spot) measurements combined with weather models, and don't capture snow depth information at appropriate scales for regional forecasting or local use. Remote sensing data have the potential to determine snow depth and other parameters for large areas that are difficult to measure directly using other methods. The Naval Postgraduate School (NPS) is using Interferometric Synthetic Aperture Radar (InSAR) to explore snow depth estimation approaches. SAR interferograms are calculated to produce digital elevation models (DEMs) for both snow-off and snow-on conditions – DEM subtraction provides an estimate of the snow depth over the area of the remotely sensed data.

Index Terms— Snow Depth, Interferometric SAR

1. INTRODUCTION

Hydrological planning, flood prediction, trafficability, avalanche control, and numerical weather/climatological modeling are among the applications that depend on reliable snow accumulation information to determine runoff. The use of remote sensing can provide information about large areas difficult to measure directly using other methods. The Naval Postgraduate School (NPS) is using Interferometric Synthetic Aperture Radar (InSAR) to explore snow depth estimation approaches. The research uses differencing of digital elevation models (DEMs) produced from airborne General Atomics Aeronautical (GAA) Ku-band Lynx SAR data [1-3]. Interferometric methods are used to generate DEMs for "snow-off" and "snow-on" conditions to determine snow depth. Other participants in this research included Sandia National Laboratory, GAA, The US Army Cold Regions Research and Engineering Laboratory (CRREL), and Mammoth Mountain California Ski Patrol. Cooperative research is also underway with the German Aerospace Center (DLR) utilizing their X-band SAR satellites (TerraSAR-X/Tandem-X). NPS also hopes to continue the research efforts utilizing a single-pass (bistatic) Ka-Band pass airborne system. The ultimate goal is to design operational approaches for regional snow depth determination using airborne and satellite SAR systems.

2. APPROACH AND METHODS

Multiple passes of the GAA airborne Ku-band Lynx SAR [3] (Table 1) were used to determine DEMs using InSAR approaches [4]. These images enabled calculation of six Snow-On and one Snow-Off interferometric pairs.

SAR Image number	Date	Time	Surface Condition
01	3 April 2012	18:47 Z, 10:47 L	snow covered
02	3 April 2012	18:55 Z, 10:55 L	snow covered
03	3 April 2012	19:04 Z, 11:04 L	snow covered
04	3 April 2012	19:00 Z, 11:00 L	snow covered
21	13 July 2012	17:58 Z, 10:58 L	bare
22	13 July 2012	18:05 Z, 11:05 L	bare

Table 1: Four usable Snow-On and two useable Snow-Off SAR images were acquired at 0.1m spatial resolution.

The Lynx radar operates at 15.2-18.2GHz (~1.8cm) to deliver multiple ground resolution options including 0.1, 0.3, 1.0, and 3.0m. For this research, 0.1m resolution Single Look Complex (SLC) SAR data were generated for each pass and spatially coregistered. SAR interferograms were produced to determine total wrapped phase, and the wrapped interferograms were unwrapped using standard approaches [4]. Because of problems calculating accurate baselines for the airborne SAR acquisitions, the flat earth correction was applied using a best-fit-plane (BFP) to the unwrapped phase (a perturbation model) and a low-resolution DEM. Phase was then converted to absolute height using linear regression to selected measured ground elevations (Figure 1).

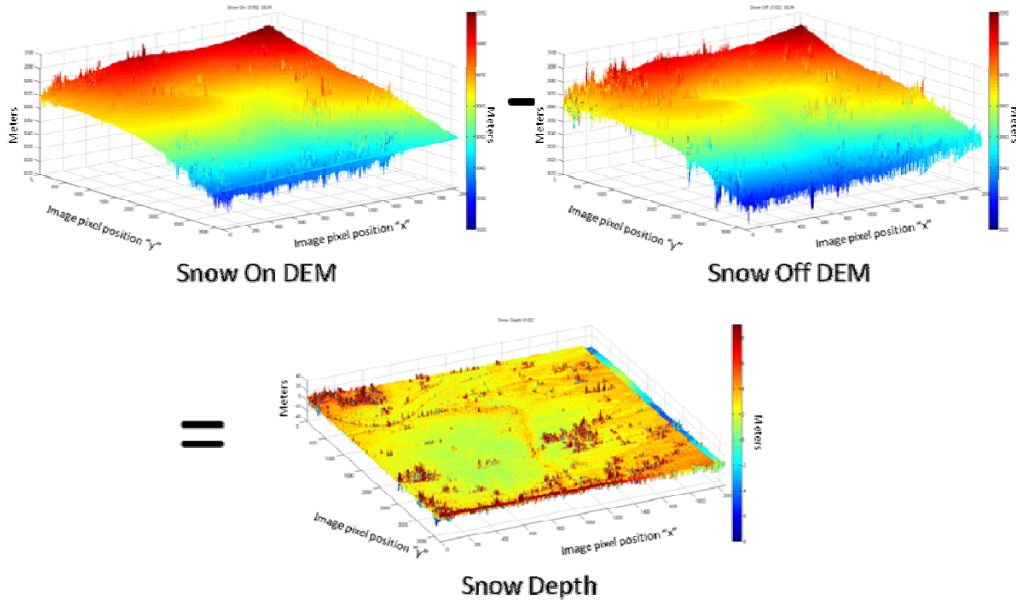♦ Current Address: HQ AFWA/A3N, USAF, Offutt Air Force Base, NE 68113

Figure 1: Top: InSAR-determined DEMs, and Bottom: results of subtracting the Snow-Off DEM from the Snow-On DEM for the Mammoth Mountain study site, (37°37.7'N, 119°02.7'N). North is to the top-center edge of the perspective view [5].

The following describes the methods used to determine and remove the best-fit-plane (BFP) from the unwrapped SAR phase [5].

An unwrapped interferogram is made up of both flat earth and terrain phase as is seen in (1) where "$\Delta\phi z$" represents the phase associated with the terrain (simplified from Richards) [4].

$$\Delta\phi_{total} = \Delta\phi_{flat\_earth} + \Delta\phi_z \qquad (1)$$

From a perturbation perspective, the flat earth phase is

$$\Delta\phi_{flat\_earth} = \Delta\bar{\phi}_{flat\_earth} + \Delta\phi'_{flat\_earth} \qquad (2)$$

The flat earth phase, however, is a plane and has no perturbation. Therefore it reduces down to

$$\Delta\phi_{flat\_earth} = \Delta\bar{\phi}_{flat\_earth} \qquad (3)$$

The terrain phase from a perturbation perspective is

$$\Delta\phi_z = \Delta\bar{\phi}_z + \Delta\phi'_z \qquad (4)$$

Unlike the flat earth phase, there are variations throughout the image. "$\overline{\Delta\phi_z}$" represents the average slope of the terrain and "$\Delta\phi_z'$" is the variation or perturbation from that average slope.

By replacing (3) and (4) into (2), the total phase can now be given as

$$\Delta\phi_{total} = \Delta\bar{\phi}_{flat\_earth} + \Delta\bar{\phi}_z + \Delta\phi'_z \qquad (5)$$

or

$$\Delta\phi_{total} = \Delta\phi_{flat\_earth} + \Delta\bar{\phi}_z + \Delta\phi'_z \qquad (6)$$

Taking the best-fit-plane of the total phase is the same as finding the average slope of the phase image and is now given by

$$\Delta\bar{\phi}_{total} = \Delta\bar{\phi}_{flat\_earth} + \Delta\bar{\phi}_z \qquad (7)$$

Subtracting the BFP or (7) from the total phase yields

$$\Delta\phi_{total} - \Delta\bar{\phi}_{total} = \Delta\phi_{flat\_earth} + \Delta\bar{\phi}_z + \Delta\phi'_z - \Delta\phi_{flat\_earth} - \Delta\bar{\phi}_z = \Delta\phi'_z \quad (8)$$

Subtracting the BFP from the total phase results in only the terrain perturbations or terrain that deviates from the mean slope, effectively separating high frequency terrain from the total phase. A BFP average slope is also determined using a low resolution DEM, which is added back to the terrain perturbations prior to snow-depth determination. Subtraction of the snow-off from the snow-on DEMs then provides an estimate of elevation change caused by snow accumulation across a SAR scene and an integrated snow volume over a specified area (Figures 1 and 2).

3. RESULTS

Snow depth was calculated using the Lynx InSAR data for a small (approximately 300 x 200m) site at Mammoth Mountain, California utilizing a snow-off DEM measured during the summer, and a total of six winter snow-on SAR image pairs at 0.1m resolution. Figure 1 shows the snow-on and snow-off DEMs and one of the snow depth results. Figure 2 shows a second InSAR-calculated snow depth image.
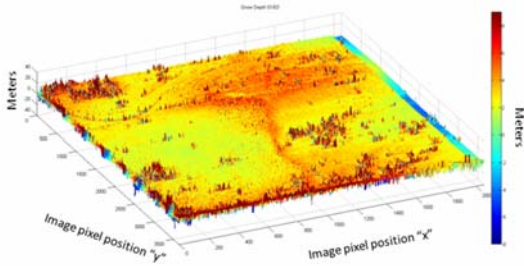
Figure 2. Snow Depth image derived from the 01/03 interferometric SAR pair, subtracted from the snow-on DEM for the Mammoth Mountain study site, (37°37.7'N, 119°02.7'N). North is to the top-center edge of the perspective view [5]. Compare to the snow depth image for pair 01/02 in Figure 1.

Most snow depths for both examples are in the 0 – 2.5m range, with some obvious errors due to the interaction of SAR with trees and other obstacles.

Manual snow depth measurements were made on a 20m grid covering the site for validation, however, because of GPS location accuracy limitations imposed on the field snow measurements, an average snow depth was calculated for a five meter radius around the recorded locations (Figure 3, right).

The SAR image pairs showed an average snow depth error of -8cm, 95cm, -49cm, 175cm 87cm and 42cm for the respective six SAR pairs (Figure 3, left). The results also indicated that coherence of the unwrapped InSAR image played a role in the DEM generation. Of the 16 manually measured locations, eight fell in a high coherence regime indicated by coherences greater than 0.7 and the others fell in a regime indicated by coherence less than 0.7. In almost all of the cases the magnitude of the error for each of the SAR image pairs fell into two categories determined by these regimes. There also appeared to be a consistent pattern of either high or low snow depth bias in the calculated snow depth results. Four of the SAR image pairs demonstrated a low average for the snow depths while the other two pairs demonstrated a high average. This pattern indicates that errors may be either related to or driven by residual slope or tilt in the BFP flat earth unwrapped interferograms. It was observed that an eastward tilt in the BFP was consistent with SAR pairs with a bias towards low snow depth errors. Those with a westward tilt demonstrated a bias towards high snow depth errors. The second bias is not as well defined, but appears to relate to coherence in the data and the range slope of the BFP. After normalizing the error there was a clear difference between the snow depth locations with high and low coherence. Additionally, the determination of whether the high or low coherence was above or below the normalization line appeared to be controlled by the range tilt of the BFP. This pattern is not fully understood, and furthermore, the observed pattern does not necessarily indicate causality. Additional SAR image pairs need to be tested to confirm the pattern. Another observation was made in four of the six SAR image pairs. It appeared that regardless of the coherence, the calculated error decreased as the observations moved southward or in the direction toward the sensor. This is indicative of a possible issue in the slope of one or more of the BFP elements. Slope issues could arise from the calculation of the BFP, accuracy of the low resolution DEM used to determine the deviation of the high frequency terrain from the average slope, or an issue with representativeness of the low resolution DEM relative to the true slope of the snow covered terrain.
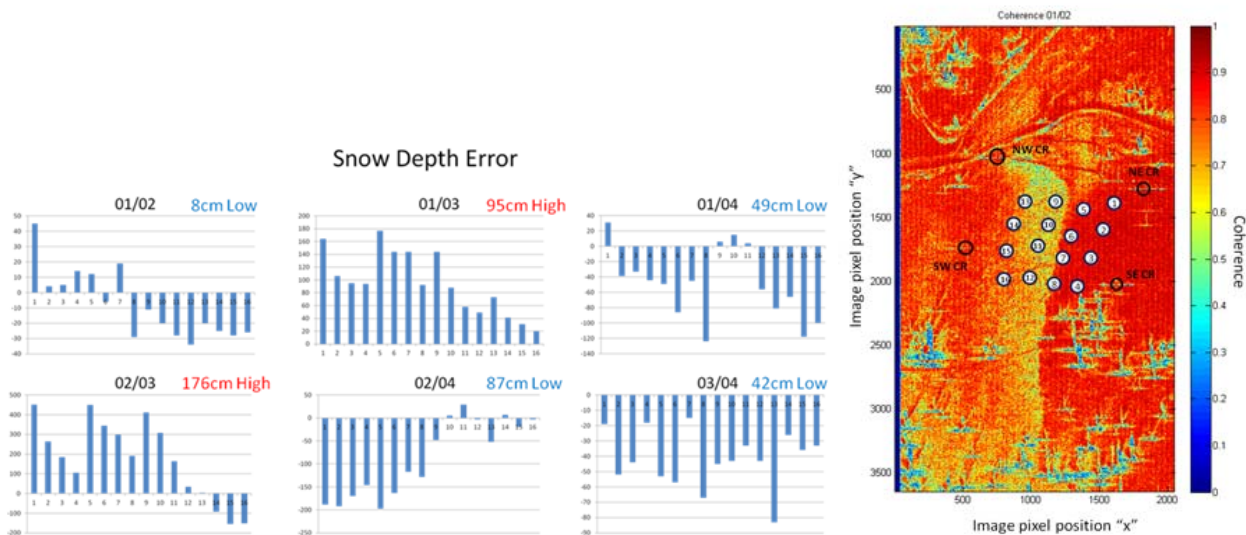

Figure 3: Left: Normalized snow depth error for each of the six interferometric image pairs for the field sites. Right: Coherence image for the 01/02 InSAR pair with the field validation snow depth sample sites marked [5].

4. CONCLUSIONS

The goal of this InSAR research was to explore the viability of using Multi-pass Single Look Complex InSAR to determine snow depth. A method was developed that removed the flat earth phase and mean slope contributions from the airborne SAR data by estimating a best-fit-plane for an unwrapped phase image combined with the average slope derived from a low-resolution DEM. The Best-fit-plane Removal (BFPR) method bypassed the requirement for detailed, precise InSAR baseline knowledge by using a perturbation or decomposition approach to isolate the interferometric phase caused by the terrain that deviated from the mean slope. After computing DEMs from both Snow-On and Snow-Off scenes they were differenced to calculate snow depth.

The snow depth results for six Snow-On InSAR pairs were compared to 16 snow depths manually measured at selected locations with varying degrees of success. The SAR image pairs showed an average error of -8cm, 95cm, -49cm, 175cm 87cm and 42cm for the respective six SAR pairs. The results also indicated that coherence of the unwrapped InSAR image played a role in the DEM generation. Of the 16 manually measured locations, eight fell in a high coherence regime indicated by coherences greater than 0.7 and the others fell in a regime indicated by coherence less than 0.7. In almost all of the cases the magnitude of the error for each of the SAR image pairs fell into two categories determined by these regimes.

There did appear to be a consistent pattern of either high or low snow depth bias in the BFPR-calculated snow depth results. Examination of biases indicates that errors may be either related to or driven by the BFPs produced from the unwrapped interferograms. There appear to be two different biases. The first is that the slope of the azimuth aspect of the BFP affects the direction of the bias. It was observed that an eastward tilt in the BFP was consistent with SAR pairs with a bias towards low snow depth errors. Those with a westward tilt demonstrated a bias towards high snow depth errors. The second bias is not as well defined, but appears to relate to coherence in the data and the range slope of the BFP. After normalizing the error there was a clear difference between the snow depth locations with high and low coherence. Additionally, the determination of whether the high or low coherence was above or below the normalization line appeared to be controlled by the range tilt of the BFP. Another observation was made in four of the six SAR image pairs. It appeared that regardless of the coherence, the calculated error decreased as the observations moved southward or in the direction toward the sensor. This is indicative of a possible issue in the slope of one or more of the BFPR elements. Slope issues could arise from the calculation of the BFP, accuracy of the low

resolution DEM used to determine the deviation of the high frequency terrain from the average slope. Despite these problems, Ku-band determined InSAR Snow-On terrain were consistently higher than Snow-Off terrain and determination of snow-depth on this basis was demonstrated. Some of the results are not fully understood and require further study. Additional SAR image pairs need to be tested to confirm patterns and observations.

5. ON-GOING RESEARCH

NPS is currently exploring the use of bistatic SAR from the German "Tandem-X" SAR system to expand the snow depth determinations to larger areas and minimize spatial and temporal baseline problems. Tandem-X snow-off and snow-on data are being acquired for the Mammoth Mountain site. Tandem-X will have the advantage of improved coherency over multiple pass (monostatic) InSAR systems, however, snow penetration will also need to be further assessed. The ultimate goal is to design operational approaches for regional snow depth determination using airborne and satellite SAR systems.

6. ACKNOWLEDGEMENTS

7. REFERENCES

[1] Evans, J. R. and Kruse, F. A., "Snow depth retrieval using Ku-Band Interferometric Synthetic Aperture Radar (InSAR)," *In Proceedings, 36th Conference on Radar Meteorology, 16-20 September 2013, Breckenridge, CO, 17 p. (2014)*

[2] Evans, J. R., Kruse, F. A., Bickel, D. L., and Dunkel, R., "Determining snow depth using Ku-Band Interferometric Synthetic Aperture Radar (InSAR)," *In Proceedings SPIE Symposium on Defense & Security, 5 - 9 May 2014, Baltimore, MD.,* (2014).

[3] Tsunoda, S. I., Pace, F., Stence, J., Woodring, M., Hensley, W. H., Doerry, A. W., and Walker, B. C., "Lynx: A high-resolution synthetic aperture radar," *Proceedings of SPIE Aerosense,* 3704, 1-8, (1999).

[4] Richards, J. A., "Remote sensing with imaging radar " *Springer-Verlag, 361 p.,* (2009).

[5] Evans, J. R., "Determining Snow Depth using Airborne Multi-Pass Interferometric Synthetic Aperture Radar, Unpublished Ph.D. Dissertation, Naval Postgraduate School, Monterey, CA, 198 p.," (2013).